Quark matter and quark stars in a quasiparticle model

Zhen Zhang,[1] Peng-Cheng Chu,[2,*] Xiao-Hua Li,[3,4,†] He Liu,[2,‡] and Xiao-Min Zhang[2,§]

[1]*Sino-French Institute of Nuclear Engineering and Technology, Sun Yat-sen University, Zhuhai 519082, China*
[2]*The Research Center for Theoretical Physics, Science School, Qingdao University of Technology, Qingdao, 266033, China*
[3]*School of Nuclear Science and Technology, University of South China, 421001 Hengyang, China*
[4]*Cooperative Innovation Center for Nuclear Fuel Cycle Technology & Equipment, University of South China, 421001 Hengyang, China*

(Received 11 January 2021; accepted 5 May 2021; published 27 May 2021)

We investigate the properties of the equation of state of strange-quark matter and *u*-*d* quark matter, the sound velocity of quark matter, the stability region for star matter, the maximum mass of quark stars (QSs), and the tidal deformability for QSs by using a quark quasiparticle model. Our results indicate that the recently discovered heavy compact stars PSR J0348 + 0432, MSR J0740 + 6620, and PSR J2215 + 5135, and especially the GW190814s secondary component m_2 can be well described as QSs within the quasiparticle model.

DOI: 10.1103/PhysRevD.103.103021

I. INTRODUCTION

The investigation of the thermodynamic properties of strongly interacting matter, especially the equation of state (EOS) of neutron star matter, is one of the fundamental issues in nuclear physics and astrophysics [1–4]. The appearance of quark matter in massive neutron stars (NSs) is considered as a hot topic in compact object studies, and NSs could be converted to strange quark stars (QSs) whose possible existence is still one of the most important fields of modern nuclear physics and astrophysics [5–11]. QSs are totally made up of strange-quark matter (SQM), which includes deconfined absolutely stable *u*, *d*, and *s* quarks with leptons in β equilibrium [7,8,12–16]. Recently, the heavy pulsar PSR J0348 + 0432 with a mass of $2.01 \pm 0.04\ M_\odot$ [17] was discovered in 2013, while the more massive compact star PSR J2215 + 5135 was detected by fitting the radial velocity lines and three-band light curves in the irradiated compact stars model, whose star mass reaches $2.27^{+0.17}_{-0.15}\ M_\odot$ [18]. In Ref. [19], using data on relativistic Shapiro delay with the Green Bank Telescope, MSR J0740 + 6620 ($2.14 \pm^{0.10}_{0.09}\ M_\odot$ with 68.3% credibility interval and $2.14 \pm^{0.20}_{0.18}\ M_\odot$ with 95.4% credibility interval) was reported as the most massive precisely observed pulsar. The observations of these supermassive compact stars can put strict constraints on the equation of state (EOS) and rule out most of the conventional phenomenological models of quark matter, whereas there exist some other models which can still describe heavy quark stars with strong isospin interactions inside the star matter [20–29].

The LIGO-Virgo Collaboration [30] detected and reported the gravitational-wave (GW) signal GW170817 from a binary compact star system, and the constraints on the thermodynamic properties of the star matter were calculated based on this observation [31–40]. In Ref. [30], the LIGO-Virgo Collaboration investigated the properties of the tidal deformability of compact stars and set an upper limit of $\Lambda_{1.4} < 800$ for the low-spin priors of 1.4 solar mass pulsars. Then, based on the upper limit for tidal deformability, constraints on the properties of the nuclear matter symmetry energy and the EOS of strongly interacting matter were calculated in numerous works [33,37,38,41–47]. In Refs. [33,48,49], $\tilde{\Lambda}$ was constrained as (0,630) for a large-spin pulsar, 300^{+420}_{-230} was obtained by considering the largest posterior density interval, and $\Lambda_{1.4} = 190^{+390}_{-120}$ was calculated using the Λm^5 linear expansion at 1.4 $M_\odot$. Furthermore, GW170817 might also have the possilility of being produced from the binary quark/hybrid star merger in Refs. [36,50,51]. Recently, the compact binary merger GW190814 [52] recently discovered by the LIGO/Virgo Collaboration, which has a secondary component m_2 with mass 2.50–2.67 $M_\odot$ at the 90% credible level, has aroused much interest in the modern physics community. Candidates for the secondary component of GW190814 include compact stars or a light black hole, and this large mass can set very strict constraints on the EOS of nuclear matter once we consider the candidate as a supermassive compact star, e.g., a quark star or a hybrid star.

*kyois@126.com
†lixiaohuaphysics@126.com
‡liuhe@qut.edu.cn
§zhangxm@mail.bnu.edu.cn

In the present work, we investigate the properties of the equation of state of SQM and u-d quark matter (udQM), the sound velocity of quark matter, the stability region for quark star matter, the maximum mass of QSs, and the tidal deformability for QSs by using the quark quasiparticle model. We find that the recently discovered supermassive compact stars can be well described as QSs within the quasiparticle model.

II. MODELS AND METHODS

A. The quasiparticle model

Unlike the conventional density-dependent quark mass model, whose equivalent quark mass includes the quark-quark effective interactions in quark matter [53–82], the equivalent mass of the quasiparticle model was derived in the zero-momentum limit of the dispersion relations by resuming one-loop self-energy diagrams in the hard dense loop approximation [83], which can be expressed as [83–85]

$$m_q = \frac{m_{q_0}}{2} + \sqrt{\frac{m_{q_0}^2}{4} + \frac{g^2\mu_q^2}{6\pi^2}}, \tag{1}$$

where m_{q0} is the quark current mass (we set $m_{u0} = 5.5$ MeV, $m_{d0} = 5.5$ MeV, and $m_{s0} = 95$ MeV in this work), μ_q represents the chemical potential of the ith flavor of quarks, and g is the strong interaction coupling constant which is treated as a free input parameter in this work.

The quasiparticle contribution to the total thermodynamic potential density for SQM can be written as

$$\Omega = \sum_i [\Omega_i + B_i(\mu_i)] + B, \tag{2}$$

where $B_i(\mu_i)$ are the additional terms introduced by medium dependence, B represents the negative vacuum pressure term for nonperturbative confinement (which can also be considered as a free input parameter) [86], and Ω_i in the sum shows the contribution to the thermodynamic potential density for all flavors of quarks (u, d, and s) and leptons (e and μ). The analytic expression for Ω_i is written as

$$\Omega_i = -\frac{g_i}{48\pi^2}\left[\mu_i\sqrt{\mu_i^2 - m_i^2}(2\mu_i^2 - 5m_i^2) + 3m_i^4 \ln\frac{\mu_i + \sqrt{\mu_i^2 - m_i^2}}{m_i^2}\right], \tag{3}$$

where g_i is the degeneracy factor with $g_i = 6$ for quarks and $g_i = 2$ for leptons. The medium-dependent term $B_i(\mu_i)$ is determined by using the integration formula as

$$B_i(\mu_i) = -\int_{m_i}^{\mu_i} \frac{\partial\Omega_i}{\partial m_i}\frac{\partial m_i}{\partial\mu_i}\mathrm{d}\mu_i. \tag{4}$$

B. Properties of strange-quark matter at zero temperature

Strange-quark matter is composed of u, d, and s quarks and leptons (e and μ) with electric charge neutrality in beta equilibrium. The weak beta-equilibrium condition at zero temperature can be written as

$$\mu_d = \mu_s = \mu_u + \mu_e, \quad \text{and} \quad \mu_\mu = \mu_e. \tag{5}$$

The electric charge neutrality condition can be expressed as

$$\frac{2}{3}n_u = \frac{1}{3}n_d + \frac{1}{3}n_s + n_e. \tag{6}$$

The total energy density $\mathcal{E}$ and the pressure P are, respectively, written as

$$\mathcal{E} = \sum_i \mathcal{E}_i = \sum_i (\Omega_i + B_i(\mu_i) + \mu_i n_i) + B, \tag{7}$$

$$P = -\sum_i (\Omega_i + B_i(\mu_i)) - B. \tag{8}$$

III. RESULTS AND DISCUSSIONS

A. The stability of SQM in QSs

In Ref. [9] the absolute stability of SQM was proposed, which requires that the minimum value of the energy per baryon of SQM at zero temperature should be less than 930 MeV [the minimum energy per baryon of the observed stable nuclei $M(^{56}\mathrm{Fe})/56$], while the minimum energy per baryon of the u-d quark matter should be larger than 930 MeV. Since ordinary nuclei are made of nucleons and not a u-d two-flavor quark phase, the energy per baryon of udQM must exceed the lowest energy per baryon found in nuclei, which is about 930 MeV for $M(^{56}\mathrm{Fe})/56$. Then, there exists no phase transition from nuclear matter to udQM, and we should use the EOS of SQM to calculate the properties of star matter. This absolutely stable condition can put very strict constraints on the parameter space for most of the phenomenological quark mass models.

In Fig. 1, we first calculate the energy per baryon and the corresponding pressure of SQM and udQM as functions of the baryon number density with four sets of parameters, i.e., $g-2$ ($g = 2, B^{1/4} = 141$ MeV), $g-3$ ($g = 3$, $B^{1/4} = 136$ MeV), $g-4$ ($g = 4$, $B^{1/4} = 131$ MeV), and $g-5$ ($g = 5$, $B^{1/4} = 120$ MeV). In our calculation, we find that the minimum energy per baryon of udQM/SQM decreases with B at a fixed coupling constant g. One can calculate the maximum mass of QSs by changing B with fixed g through using the EOS of SQM under the absolute stability condition. For example, for the $g = 2$ case, the minimum energy per baryon of SQM/udQM reaches 930/1014 MeV with $B^{1/4} = 153$ MeV, while the minimum energy per

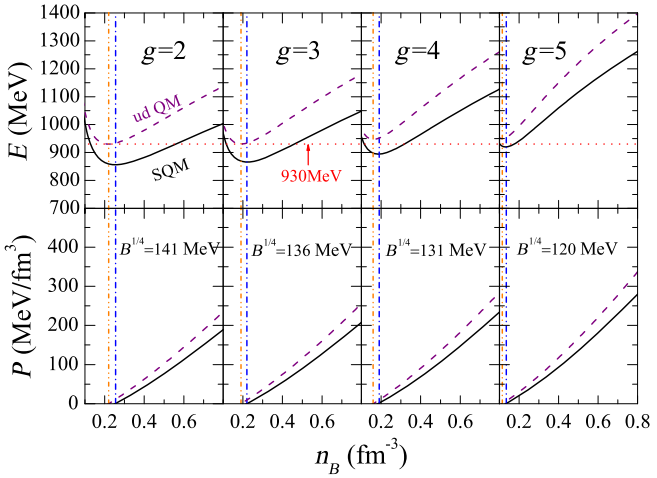

FIG. 1. Energy per baryon and the corresponding pressure as functions of the baryon density for SQM and udQM within the quasiparticle model with different parameter sets at zero temperature.

baryon of SQM/udQM decreases to 856/930 MeV with $B^{1/4} = 141$ MeV. The parameter sets $g-2$, $g-3$, $g-4$, and $g-5$ in Fig. 1 are chosen under the stability condition, where we change B to obtain 2.01, 2.14, 2.27, and 2.59 solar mass QSs at a certain coupling constant g ($g = 2, 3, 4, 5$). One can find that all of the minimum values of the energy per baryon for SQM/udQM from these four cases are smaller/larger than 930 MeV, which satisfies the absolutely stable conditions for SQM and udQM. Furthermore, it can be seen from Fig. 1 that the baryon density of the minimum energy per baryon for SQM and udQM in the four cases is exactly the corresponding zero pressure baryon density, which meets the requirement of thermodynamical self-consistency for quark matter. In particular, we find that the value of the zero-pressure density of SQM (udQM) decreases from 0.255 (0.22) fm^{-3} to 0.135 (0.115) fm^{-3} when g increases from 2 to 5, and the minimum value of the energy per baryon for SQM and udQM increases with the increment of the coupling constant g. The correlation between g and the energy per baryon of quark matter can also be found in Ref. [83], while the energy density of quark matter seems to have no dependence on the constant g in Fig. 7 of Ref. [83]. We mention that the energy density in Fig. 7 of Ref. [83] is not based on the β-equilibrium condition of strange quark matter in QSs, and the results from Figs. 5–7 in that work focus on the correlation between the energy density at the baryon density of the minimum energy per baryon and a constant g with other parameters being fixed (the results we show in Fig. 1 of our work are the energy per baryon as a function of the baryon density under the β-equilibrium condition with different sets of parameters). We then calculate the energy density at the baryon density of the minimum energy per baryon under the same conditions as in Ref. [83] with different values of g, and the results show that the energy density can also stay approximately constant, which does not contradict the results of Ref. [83]. Moreover, one can see from Fig. 1 that the pressure and energy per baryon for the SQM and udQM cases both increase with g, which implies that the EOS for large g can support heavier QSs within the quasiparticle bag model. In addition, we also check the phase transition from nuclear matter to udQM by using the quasiparticle model (for quark phase) and the MDI model (the MDI model is an isospin- and momentum-dependent effective nuclear interaction model [87], which is used for the hadron phase in this work). Generally, the hadron-quark phase transition from nuclear matter to quark matter might appear at 3–5 times the saturation density ρ_0 in the hybrid star approach, and this phase transition usually moves to a higher density region with increasing stiffness of the EOS of the quark matter. In this work, we use the Gibbs construction method to construct the hadron-quark mixed phase, and we find that the phase transition from nuclear matter to udQM appears at $n_B = 1.25$ fm^{-3} when $g-5$ is chosen for udQM, which is much larger than the saturation density and implies that the phase transition from the nuclear phase to the quark phase does not occur too early. In the mixed phase, the phase transition softens the EOSs, which causes the udQM to appear at very high baryon density (larger than 2.5 fm^{-3}). In the present work, we employ the MDI model to describe the hadron phase for simplicity, and more systematic investigations on the hadron-quark phase transition with the quasiparticle model and other phenomenological models for nuclear matter (e.g., the constraints on the EOSs from models of nuclear matter in Ref. [88]) will be further studied in future work.

In addition, we also examine the sound velocity in Fig. 2 by using $c_s^2 = \partial P/\partial E$ within the quasiparticle model with $g-2$, $g-3$, $g-4$, and $g-5$ at zero temperature, and we

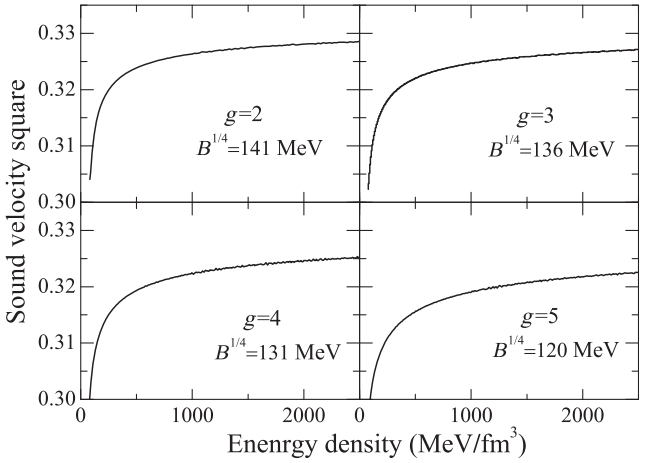

FIG. 2. Sound velocity squared as a function of the energy density for SQM within the quasiparticle model with $g-2$, $g-3$, $g-4$, and $g-5$ at zero temperature.

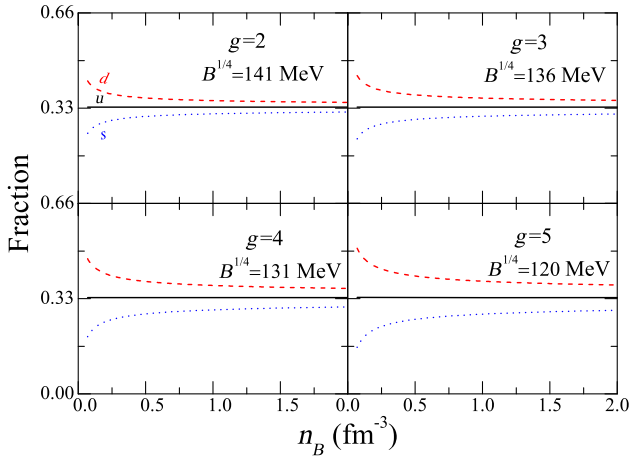

FIG. 3. Quark fraction as a function of the baryon density in SQM with $g-2$, $g-3$, $g-4$, and $g-5$ at zero temperature.

obtain that the sound velocity is less than the speed of light in all four cases, which satisfies the causality condition $c_s < c$. One can also find in Fig. 2 that the sound velocity squared decreases with the increment of g.

In Fig. 3, we calculate the quark fraction as a function of the baryon density in SQM with $g-2$, $g-3$, $g-4$, and $g-5$ at zero temperature, and one can find that the difference among the fractions of u, d, and s quarks decreases with the baryon density. In particular, it is interesting to see that the difference of the quark fraction becomes larger once g increases, which indicates that the u-d quark isospin asymmetry $\delta = 3(n_d - n_u)/(n_d + n_u)$ increases as the coupling constant g increases in SQM.

In Fig. 4, we calculate the mass-radius relation of QSs with $g-2$, $g-3$, $g-4$, and $g-5$. The large compact star mass value $2.59^{+0.08}_{-0.09}$ $M_\odot$(90%C.L.) from GW190814 [52], the two independent constraints of the simultaneous M-R measurements from NICER (through the analysis of the

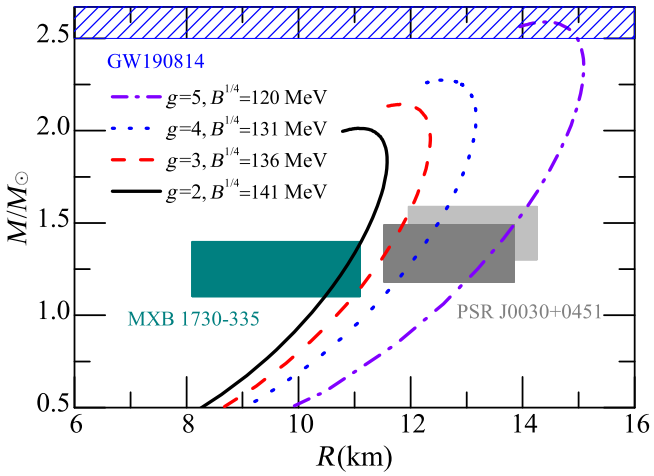

FIG. 4. Mass-radius relation of QSs with $g-2$, $g-3$, $g-4$, and $g-5$ at zero temperature.

x-ray data for the millisecond pulsar PSR J0030 + 451) [89,90], and the mass and radius regions of the pulsars in the rapid burster MXB 1730-335 using the analysis of Swift/XRT time-resolved spectra of the burst [91] are all included in this figure for comparison. It can be seen that the results of the maximum mass of QSs with $g-2$ and $g-3$ are both consistent with the observations of the pulsars in the rapid burster MXB 1730-335 and can describe PSR J0348 + 0432 with a mass of 2.01 ± 0.04 $M_\odot$ [17] and the recently discovered massive pulsar MSR J0740 + 6620 ($2.14 \pm^{0.10}_{0.09}$ $M_\odot$ at the 68.3% credibility interval and $2.14 \pm^{0.20}_{0.18}$ $M_\odot$ at the 95.4% credibility interval) [19] as QSs. Furthermore, the results of the maximum mass of QSs with $g-3$, $g-4$, and $g-5$ are all consistent with the constraints from NICER, and one can describe PSR J2215 + 5135 with a mass of $2.27 \pm^{0.10}_{0.09}$ $M_\odot$ as QSs with $g-4$. For the case $g-5$, one can find that the maximum mass of the QSs is 2.59 $M_\odot$, which can describe the GW190814's secondary component as QSs within the quasiparticle model. Additionally, the results show that the EOS of the large QSs whose maximum mass exceeds two solar masses with large radii cannot fulfill the MXB constraint, which implies that MXB1730-355 might belong to another branch of stars proposed in the so-called two-families scenario from Ref. [92].

To further check the effects of the coupling constant g and search for the maximum mass range of QSs by considering the absolutely stable condition within the quasiparticle model, we calculate the maximum mass of QSs as a function of the coupling constant g by satisfying the absolutely stable condition in Fig. 5. In this figure, the allowed values of the maximum mass of QSs and the coupling constant g within the quasiparticle model are chosen in the stability window of SQM (shaded area), where the maximum mass and parameter sets are all able to fulfill the absolutely stable condition. The star mass constraints from PSR J0348 + 0432, MSR J0740 + 6620, PSR J2215 + 5135, and GW190814 are also listed in Fig. 5, and one can find that the allowed ranges of the coupling constant g are (2,3.58), (2.92,4), (3.58,4.36), and (4.62,5.03) for these four star mass constraints, respectively. We also mention that the range of the maximum mass of QSs decreases with the increment of the coupling constant g in the stability window of SQM, and the range finally narrows down to a "point" when the maximum mass of QSs within the quasiparticle model reaches 3.03 solar masses, where the coupling constant g increases to 5.6. In Fig. 6, we calculate the energy per baryon and the corresponding pressure as functions of the baryon density for SQM and u-d quark matter with $g = 5.6$ within the quasiparticle model. One can see that the minimum values of the energy per baryon for SQM and udQM are exactly equal to 930 MeV, which indicates the maximum value of the coupling constant g by considering the stability condition of SQM within the quasiparticle model. Therefore, our

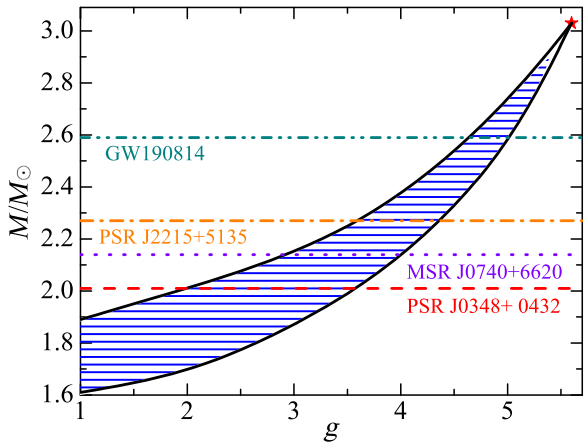

FIG. 5. Maximum mass of QSs as functions of the coupling constant g by satisfying the absolutely stable condition within the quasiparticle model.

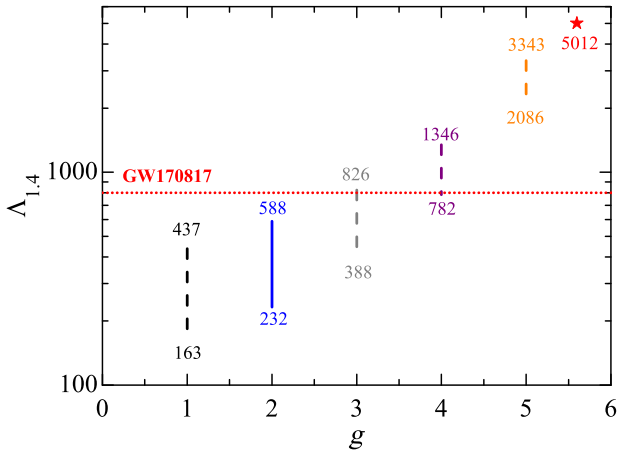

FIG. 7. Dimensionless tidal deformability $\Lambda_{1.4}$ as a function of the coupling constant g by considering the absolutely stable condition in SQM. The red dotted line denotes the $\Lambda_{1.4} < 800$ upper limit derived from GW170817.

results show that the maximum mass of QSs within the quasiparticle model by considering the stability condition of SQM is 3.03 solar masses, and the corresponding coupling constant g also reaches the maximum value $g = 5.6$, which can be considered as the extreme cases for the parameter sets in this model.

The observation of tidal effects in binary compact star systems can provide significant information about the thermodynamic properties of the star matter because of the tidal deformation being determined by the internal structure of the compact stars. In Fig. 7, we calculate the dimensionless tidal deformability $\Lambda_{1.4}$ as a function of the coupling constant g by considering the absolutely stable condition in SQM. The upper limit $\Lambda_{1.4} < 800$ derived from GW170817 is also listed in order to check if this constraint is violated in the large value area of the maximum mass of QSs

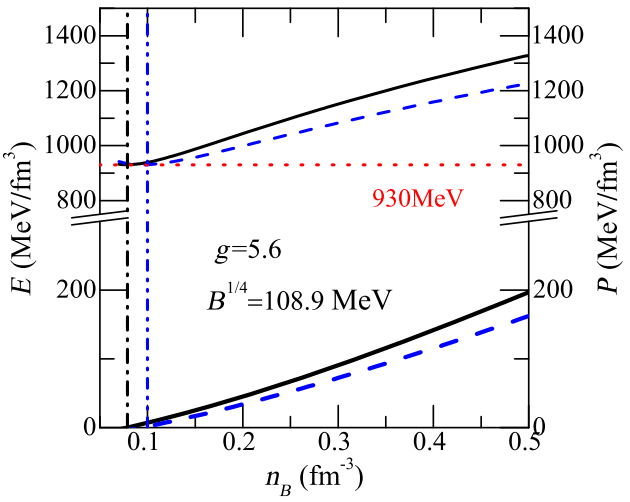

FIG. 6. Energy per baryon and the corresponding pressure as functions of the baryon density for SQM and udQM within the quasiparticle model with $g = 5.6$ at zero temperature.

and the coupling constant g. Based on the absolutely stable condition, the tidal deformability $\Lambda_{1.4}$ is constrained within a certain range with the fixed coupling constant g. One can find from Fig. 7 that $\Lambda_{1.4}$ increases from 163 to 437 with $(g = 1, B^{1/4} \in (143, 158)$ MeV) and 232 to 588 with $(g = 2, B^{1/4} \in (141, 153)$ MeV) in order to satisfy the absolutely stable condition, while for the $(g = 3, B^{1/4} \in (136, 147)$ MeV), $(g = 4, B^{1/4} \in (128, 137)$ MeV), and $(g = 5, B^{1/4} \in (117, 121)$ MeV) cases, $\Lambda_{1.4}$ increases from 388 to 826, 782 to 1346, and 2086 to 3343. It can be seen that $\Lambda_{1.4}$ for the $(g = 1, B^{1/4} \in (143, 158)$ MeV) and $(g = 2, B^{1/4} \in (141, 153)$ MeV) cases is totally below the upper limit $\Lambda_{1.4} < 800$ derived from GW170817, while the tidal deformability ranges for the $(g = 3, B^{1/4} \in (136, 147)$ MeV) and $(g = 4, B^{1/4} \in (128, 137)$ MeV) cases both partly exceed the upper limit $\Lambda_{1.4} = 800$ when $(B^{1/4} = 145, M_{QS} = 2.12\ M_\odot)$ and $(B^{1/4} = 129, M_{QS} = 2.13\ M_\odot)$ for $g = 3$ and $g = 4$, respectively. In particular, the tidal deformability for the $(g = 5, B^{1/4} \in (117, 121)$ MeV) case completely exceeds the upper limit constraint from GW170817. For the extreme case $(g = 5.6, B^{1/4} = 108.9$ MeV), $\Lambda_{1.4}$ reaches 5012, which strongly violates the constraint $\Lambda_{1.4} < 800$ derived from GW170817. Finally, our results above indicate that we cannot describe GW170817 as QSs whose maximum mass is larger than 2.13 $M_\odot$ within the quasiparticle model, and the candidates for GW170817 might be neutron stars (if the flux of strangelets produced in the merger of quark stars is suppressed or strangelets evaporate or decay [93,94]) or quark stars.

B. Discussion on the coupling constant g

In the previous subsection, we discussed the properties of SQM and QSs within the quasiparticle model by treating

the coupling constant g as fixed, and this treatment can be found in many works [79,83,85,95]. In principle, the running coupling constant should not be fixed and the effective quark mass should decrease with increasing μ_i in the large baryon density region to satisfy the restoration of chiral symmetry from the QCD features. To fix this problem, an effective running coupling constant $g^2(\mu_i) = \frac{48\pi^2}{29}[\ln(\frac{0.8\mu_i^2}{\Lambda^2})]^{-1}$ was proposed in Refs. [96–98] with the QCD scale-fixing parameter Λ taken to be 120–200 MeV.

In Fig. 8, we calculate the effective quark mass as a function of the baryon density with the fixed coupling constant and effective running coupling constant within the quasiparticle model. In the first panel, the parameters are set as $g-5$ ($g=5$, $B^{1/4}=120$ MeV), which is the fixed coupling constant case, and one can see that the effective quark masses for u, d, and s quarks all increase with the baryon density. From Eq. (1) one can easily find that the quark mass increases with the chemical potential at zero temperature for the fixed coupling constant case, which cannot provide the chiral symmetry restoration within the quasiparticle model. In the upper-right panel of Fig. 8, we calculate the quark mass by using the effective running coupling constant

$$g^2(\mu_i) = \frac{48\pi^2}{29}\left[\ln\left(\frac{0.8\mu_i^2}{\Lambda^2}\right)\right]^{-1}, \tag{9}$$

where Λ is set to 200 MeV and $B^{1/4}=120$ MeV. One can find that the quark masses of all three flavors of quarks first decrease with the baryon density from 0.1–0.4 fm^{-3}, and then increase with the baryon density in this treatment, which still cannot satisfy the QCD features due to the increment of the quark mass [from Eq. (1)] with the chemical potential in the ultrahigh-density region.

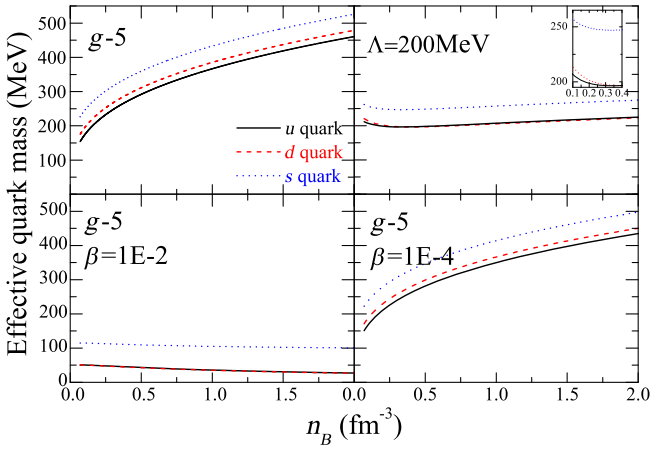

FIG. 8. Quark mass as a function of baryon density with the fixed coupling constant and effective running coupling constant within the quasiparticle model.

In order to solve the restoration of chiral symmetry for the effective quark mass within the quasiparticle model, one should build a new form of the effective running coupling constant g. Because of the complexity and difficulty in the straight calculation of the effective running coupling constant, we rewrite g for simplicity by using the phenomenological approach,

$$g^2(\mu_i) \to g^2 e^{-\beta\mu_i}, \tag{10}$$

where β is a parameter determining the chemical potential dependence of the effective running coupling constant. This chemical-potential-dependent quark mass coupling constant is similar to the treatment of Ref. [80] within the CIDDM model. One can see that the restoration of chiral symmetry can be guaranteed if $\beta > 0$, and we believe that more formal and reasonable treatments for the effective running coupling constant g within the quasiparticle model can be proposed in future works. In this work, we use Eq. (10) and set $g=5$, $B^{1/4}=120$ MeV to calculate the effective quark mass in the lower-left ($\beta=0.01$) and lower-right ($\beta=0.0001$) panels in Fig. 8. One can find in the lower-left panel that the quark masses of all flavors of quarks decrease with the increment of baryon density, and the effective quark mass can decrease to its current mass when $n_B = 2$ fm^{-3}. One can also find in the lower-right panel of Fig. 8 that the values of the effective quark mass for the quark star matter region (the maximum value of the baryon density for the quark star matter region is the central baryon density of the maximum mass of QSs, which usually appears around $n_B = 1$ fm^{-3}) seems to be almost identical to the quark mass in the fixed coupling constant case once β is set very small, e.g., $\beta=0.0001$. This result indicates that we can still use the conclusions from the fixed coupling constant case in the quark star matter region once

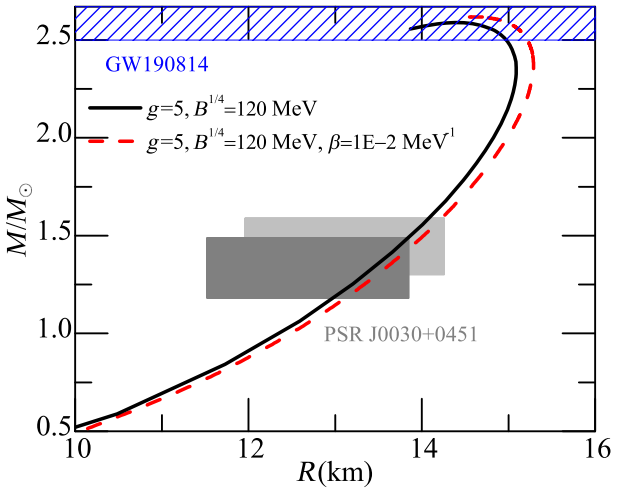

FIG. 9. Mass-radius relation with the fixed coupling constant and effective running coupling constant within the quasiparticle model.

β is set extremely small, and the effective quark mass in this case can still satisfy the restoration of chiral symmetry at ultrahigh baryon density.

Additionally, we calculate the mass-radius relation with the effective running coupling constant $g^2(\mu_i) \to g^2 e^{-\beta\mu_i}$ within the quasiparticle model. One can find in Fig. 9 that the maximum mass of QSs reaches 2.62 $M_\odot$ with $g = 5$, $B^{1/4} = 120$ MeV, and $\beta = 0.01$, which is approximately identical to the maximum quark star mass in the $g - 5$ case with the fixed coupling constant g (2.59 solar masses) and can still describe GW190814's secondary component as QSs within the quasiparticle model.

IV. CONCLUSION AND DISCUSSION

In this work, we have explored the properties of the EOSs of SQM and udQM, the sound velocity of quark matter, the quark fraction, the maximum mass of QSs and the coupling constant g, as well as the tidal deformability for QSs by using the quark quasiparticle model. Our results show that we can describe the recently discovered heavy compact stars, especially GW190814's secondary component, as QSs within the quasiparticle model.

In order to satisfy the absolutely stable condition for SQM, we further studied the range of the maximum mass of QSs and the parameter sets. We found that the range of the maximum mass of QSs decreases with the increment of the coupling constant g when the absolutely stable condition is considered, and the heaviest QSs that the quasiparticle model can support are of 3.03 solar masses.

Moreover, we also calculated the tidal deformability of QSs in the stability window of SQM. We found that the tidal deformability of the large-mass QSs can violate the upper limit constraint $\Lambda_{1.4} < 800$ derived from GW170817 for large-mass stars within the quasiparticle model. Furthermore, we discussed the expressions of the effective coupling constant g, and we used a phenomenological approach to temporarily solve the restoration of chiral symmetry for the effective quark mass within the quasiparticle model.

Therefore, our results have demonstrated that we can describe newly discovered heavy compact stars as QSs by using the quasiparticle model, and the absolutely stable condition for SQM indeed puts very strict constraints on the range of the parameter sets, the maximum mass of QSs, and the tidal deformability of QSs. In particular, our results have shown that the maximum mass of QSs that the quasiparticle model can support is 3.03 solar masses, and the tidal deformability $\Lambda_{1.4}$ for large QSs can violate the upper limit from GW170817.

ACKNOWLEDGMENTS

This work is supported by the NSFC under Grants No. 11975132, 11905302, 11505100, and 11605100, and the Shandong Provincial Natural Science Foundation, China ZR2019YQ01 and ZR2015AQ007.

[1] N. K. Glendenning, *Compact Stars*, 2nd ed. (Spinger-Verlag Inc., New York, 2000).
[2] F. Weber, *Pulsars as Astrophyical Laboratories for Nuclear and Particle Physics* (IOP Publishing Ltd, London, UK, 1999).
[3] J. M. Lattimer and M. Prakash, Science **304**, 536 (2004).
[4] A. W. Steiner, M. Prakash, J. M. Lattimer, and P. J. Ellis, Phys. Rep. **411**, 325 (2005).
[5] D. Ivanenko and D. F. Kurdgelaidze, Lett. Nuovo Cimento **2**, 13 (1969).
[6] N. Itoh, Prog. Theor. Phys. **44**, 291 (1970).
[7] A. R. Bodmer, Phys. Rev. D **4**, 1601 (1971).
[8] E. Witten, Phys. Rev. D **30**, 272 (1984).
[9] E. Farhi and R. L. Jaffe, Phys. Rev. D **30**, 2379 (1984).
[10] C. Alcock, E. Farhi, and A. Olinto, Astrophy. J. **310**, 261 (1986).
[11] F. Weber, Prog. Part. Nucl. Phys. **54**, 193 (2005).
[12] I. Bombaci, I. Parenti, and I. Vidana, Astrophy. J. **614**, 314 (2004).
[13] J. Staff, R. Ouyed, and M. Bagchi, Astrophy. J. **667**, 340 (2007).
[14] M. Herzog and F. K. Röpke, Phys. Rev. D **84**, 083002 (2011).
[15] M. A. Stephanov, K. Rajagopal, and E. V. Shuryak, Phys. Rev. Lett. **81**, 4816 (1998).
[16] H. Terazawa, INS-Report, Report No. 336, University of Tokyo, 1979.
[17] J. Antoniadis *et al.*, Science **340**, 1233232 (2013).
[18] M. Linares, T. Shahbaz, and J. Casares, Astrophys. J. **859**, 54 (2018).
[19] H. T. Cromartie *et al.*, Nat. Astron. **4**, 72 (2020); Nat. Astron. **4**, 72 (2019).
[20] M. Alford and S. Reddy, Phys. Rev. D **67**, 074024 (2003).
[21] M. Alford, P. Jotwani, C. Kouvaris, J. Kundu, and K. Rajagopal, Phys. Rev. D **71**, 114011 (2005).
[22] M. Baldo, Phys. Lett. B **562**, 153 (2003).
[23] N. D. Ippolito, M. Ruggieri, D. H. Rischke, A. Sedrakian, and F. Weber, Phys. Rev. D **77**, 023004 (2008).
[24] X. Y. Lai and R. X. Xu, Res. Astron. Astrophys. **11**, 687 (2011).
[25] M. G. B. de Avellar, J. E. Horvath, and L. Paulucci, Phys. Rev. D **84**, 043004 (2011).
[26] L. Bonanno and A. Sedrakian, Astron. Astrophys. **539**, A16 (2012).
[27] P. C. Chu, B. Wang, Y.-Y. Jia, Y.-M. Dong, S.-M. Wang, X.-H. Li, L. Zhang, X.-M. Zhang, and H.-Y. Ma, Phys. Rev. D **94**, 123014 (2016).

[28] P. C. Chu, X.-H. Li, B. Wang, Y.-M. Dong, Y.-Y. Jia, S.-M. Wang, and H.-Y. Ma, Eur. Phys. J. C **77**, 512 (2017).
[29] P. C. Chu, Y. Zhou, C. Chen, X.-H. Li, and H.-Y. Ma, J. Phys. G, Nucl. Part. Phys. **47**, 085201 (2020).
[30] B. P. Abbott *et al.*, Phys. Rev. Lett. **119**, 161101 (2017).
[31] L. Rezzolla, E. R. Most, and L. R. Weih, Astrophys. J. Lett. **852**, L25 (2018).
[32] E. R. Most, L. R. Weih, L. Rezzolla, and J. Schaffner-Bielich, Phys. Rev. Lett. **120**, 261103 (2018).
[33] Y. Zhou, L.-W. Chen, and Z. Zhang, Phys. Rev. D **99**, 121301(R) (2019).
[34] A. Bauswein, O. Just, H.-T. Janka, and N. Stergioulas, Astrophys. J. Lett. **850**, L34 (2017).
[35] B. Margalit and B. D. Metzger, Astrophys. J. Lett. **850**, L19 (2017).
[36] E. Zhou, X. Zhou, and A. Li, Phys. Rev. D **97**, 083015 (2018).
[37] F. J. Fattoyev, J. Piekarewicz, and C. J. Horowitz, Phys. Rev. Lett. **120**, 172702 (2018).
[38] E. Annala, T. Gorda, A. Kurkela, and A. Vuorinen, Phys. Rev. Lett. **120**, 172703 (2018).
[39] D. Radice, A. Perego, F. Zappa, and S. Bernuzzi, Astrophys. J. Lett. **852**, L29 (2018).
[40] M. Ruiz, S. L. Shapiro, and A. Tsokaros, Phys. Rev. D **97**, 021501(R) (2018).
[41] J.-E. Christian, A. Zacchi, and J. Schaffner-Bielich, Phys. Rev. D **99**, 023009 (2019).
[42] G. Montana, L. Tolos, M. Hanauske, and L. Rezzolla, Phys. Rev. D **99**, 103009 (2019).
[43] P. C. Chu, L. W. Chen, and X. Wang, Phys. Rev. D **90**, 063013 (2014).
[44] P. C. Chu, Y. Zhou, X. Qi, X.-H. Li, Z. Zhang, and Y. Zhou, Phys. Rev. C **99**, 035802 (2019).
[45] P. C. Chu, Y. Zhou, X.-H. Li, and Z. Zhang, Phys. Rev. D **100**, 103012 (2019).
[46] P. C. Chu, Y. Zhou, Y.-Y. Jiang, H.-Y. Ma, H. Liu, X.-M. Zhang, and X.-H. Li, Eur. Phys. J. C **81**, 93 (2021).
[47] N. B. Zhang and B. A. Li, Astrophys. J. **879**, 99 (2019).
[48] B. P. Abbott *et al.* (The LIGO Scientific and the Virgo Collaborations), Phys. Rev. X **9**, 011001 (2019).
[49] B. P. Abbott *et al.*, Phys. Rev. Lett. **121**, 161101 (2018).
[50] R. Nandi and P. Char, Astrophys. J. **857**, 12 (2018).
[51] V. Paschalidis, K. Yagi, D. Alvarez-Castillo, D. B. Blaschke, and A. Sedrakian, Phys. Rev. D **97**, 084038 (2018).
[52] R. Abbott *et al.*, Astrophys. J. Lett. **896**, L44 (2020).
[53] A. Chodos, R. L. Jaffe, K. Ohnson, C. B. Thorn, and V. F. Weisskopf, Phys. Rev. D **9**, 3471 (1974).
[54] M. Alford, M. Braby, M. Paris, and S. Reddy, Astrophy. J. **629**, 969 (2005).
[55] J. Y. Chao, P. Chu, and M. Huang, Phys. Rev. D **88**, 054009 (2013).
[56] P. C. Chu, X. Wang, L.-W. Chen, and M. Huang, Phys. Rev. D **91**, 023003 (2015).
[57] P. C. Chu, B. Wang, H.-Y. Ma, Y.-M. Dong, S.-L. Chang, C.-H. Zheng, J.-T. Liu, and X.-M. Zhang, Phys. Rev. D **93**, 094032 (2016).
[58] P. C. Chu and L.-W. Chen, Phys. Rev. D **96**, 083019 (2017).
[59] P. Rehberg, S. P. Klevansky, and J. Hüfner, Phys. Rev. C **53**, 410 (1996).
[60] M. Hanauske, L. M. Satarov, I. N. Mishustin, H. Stocker, and W. Greiner, Phys. Rev. D **64**, 043005 (2001).
[61] S. B. Rüster and D. H. Rischke, Phys. Rev. D **69**, 045011 (2004).
[62] D. P. Menezes, C. Providencia, and D. B. Melrose, J. Phys. G **32**, 1081 (2006).
[63] C. D. Roberts and A. G. Williams, Prog. Part. Nucl. Phys. **33**, 477 (1994) and references therein.
[64] H. S. Zong, L. Chang, F. Y. Hou, W. M. Sun, and Y. X. Liu, Phys. Rev. C **71**, 015205 (2005).
[65] S. X. Qin, L. Chang, H. Chen, Y. X. Liu, and C. D. Roberts, Phys. Rev. Lett. **106**, 172301 (2011).
[66] B. A. Freedman and L. D. Mclerran, Phys. Rev. D **16**, 1169 (1977).
[67] E. S. Fraga, R. D. Pisarski, and J. Schaffner-Bielich, Phys. Rev. D **63**, 121702(R) (2001).
[68] E. S. Fraga and P. Romatschke, Phys. Rev. D **71**, 105014 (2005).
[69] A. Kurkela, P. Romatschke, and A. Vuorinen, Phys. Rev. D **81**, 105021 (2010).
[70] G. N. Fowler, S. Raha, and R. M. Weiner, Z. Phys. C **9**, 271 (1981).
[71] S. Chakrabarty, S. Raha, and B. Sinha, Phys. Lett. B **229**, 112 (1989).
[72] S. Chakrabarty, Phys. Rev. D **43**, 627 (1991); **48**, 1409 (1993); **54**, 1306 (1996).
[73] O. G. Benvenuto and G. Lugones, Phys. Rev. D **51**, 1989 (1995).
[74] G. X. Peng, H. C. Chiang, J. J. Yang, L. Li, and B. Liu, Phys. Rev. C **61**, 015201 (1999).
[75] G. X. Peng, H. C. Chiang, B. S. Zou, P. Z. Ning, and S. J. Luo, Phys. Rev. C **62**, 025801 (2000).
[76] G. X. Peng, A. Li, and U. Lombardo, Phys. Rev. C **77**, 065807 (2008).
[77] A. Li, G. X. Peng, and J. F. Lu, Res. Astron. Astrophys. **11**, 482 (2011).
[78] K. Schertler, C. Greiner, and M. H. Thoma, Nucl. Phys. **A616**, 659 (1997).
[79] K. Schertler, C. Greiner, P. K. Sahu, and M. H. Thoma, Nucl. Phys. **A637**, 451 (1998).
[80] P. C. Chu and L. W. Chen, Astrophys. J. **780**, 135 (2014).
[81] P. C. Chu, X.-H. Li, H.-Y. Ma, B. Wang, Y.-M. Dong, and X.-M. Zhang, Phys. Lett. B **778**, 447 (2018).
[82] P. C. Chu and L. W. Chen, Phys. Rev. D **96**, 103001 (2017).
[83] K. Schertler, C. Greiner, and M. H. Thoma, Nucl. Phys. **A616**, 659 (1997).
[84] R. D. Pisarski, Nucl. Phys. **A498**, 423 (1989).
[85] X. J. Wen *et al.*, J. Phys. G, Nucl. Part. Phys. **36**, 025011 (2009).
[86] B. K. Patra and C. P. Singh, Phys. Rev. D **54**, 3551 (1996).
[87] J. Xu, L.-W. Chen, and B.-A. Li, Phys. Rev. C **91**, 014611 (2015).
[88] P. Danielewicz *et al.*, Science **298**, 1592 (2002).
[89] T. E. Riley *et al.*, Astrophys. J. Lett. **887**, L21 (2019).
[90] M. C. Miller *et al.*, Astrophys. J. Lett. **887**, L24 (2019).
[91] G. Sala, F. Haberl, J. Jose, A. Parikh, R. Longland, L. C. Pardo, and M. Andersen, Astrophys. J. **752**, 158 (2012).

[92] A. Drago, A. Lavagno, and G. Pagliara, Phys. Rev. D **89**, 043014 (2014).
[93] J. E. Horvath, O. G. Benvenuto, E. Bauer, L. Paulucci, A. Bernardo, and H. R. Viturro, Universe **5**, 144 (2019).
[94] N. Bucciantini *et al.*, arXiv:1908.02501.
[95] X. J. Wen, Physica (Amsterdam) **392A**, 392, 4388 (2013).
[96] X. J. Wen, J. Y. Li, J. Q. Liang, and G. X. Peng, Phys. Rev. C **82**, 025809 (2010).
[97] X. J. Wen, S.-Z. Su, D.-H. Yang, and G.-X. Peng, Phys. Rev. D **86**, 034006 (2012).
[98] B. K. Patra and C. P. Singh, Phys. Rev. D **54**, 3551 (1996).